# *Ab initio* calculations of magnetotransport for magnetic multilayers

C. Blaas and P. Weinberger
*Center for Computational Materials Science and Institut für Technische Elektrochemie und Festkörperchemie, Technische Universität Wien, 1060 Vienna, Austria*

L. Szunyogh
*Center for Computational Materials Science, 1060 Vienna, Austria and Department of Theoretical Physics, Technical University Budapest, 1521 Budapest, Hungary*

P. M. Levy
*Department of Physics, New York University, New York, New York 10003*

C. B. Sommers
*Laboratoire de Physique des Solides, Université de Paris–Sud, 91405 Orsay, France*
(Received 8 February 1999)

We have used the spin-polarized relativistic screened Korringa-Kohn-Rostoker method for layered systems together with the Kubo-Greenwood formalism and the coherent-potential approximation to describe electrical transport properties of magnetic multilayers. We are able to calculate resistivities and magnetoresistance of model structures with no adjustable parameters by simultaneously determining contributions to the giant magnetoresistance of multilayers coming from both the electronic structure and spin-dependent scattering off impurities. [S0163-1829(99)05125-5]

## I. INTRODUCTION

The giant magnetoresistance (GMR) displayed by magnetic multilayers has been attributed to the spin dependence of both the electronic structure, due to the background or intrinsic potential of an array of atoms, and to the scattering from defects.[1] Several *ab initio* or first-principles calculations have assessed the role of the spin dependence of the electronic structure in producing the GMR observed in multilayers; they come in two varieties: for periodic structures, superlattices,[2–6] and potential steps at the interface between magnetic and nonmagnetic layers.[7] Both seem to be on firm footing, and there is a consensus that these *ab initio* calculations accurately portray the contributions of the electronic structure to GMR. While there have been realistic calculations of the spin-dependent scattering from isolated impurities,[4] *ab initio* calculations of the role of defects in producing GMR have been less successful up till now. If we focus on the scattering from impurities what is lacking at this time is an *ab initio* scheme which *simultaneously* evaluates the GMR arising from the electronic structure and concentrated impurities.

By using the nonrelativistic layer Korringa-Kohn-Rostoker (KKR) code developed by MacLaren[8] and the local spin-density approximation (LSDA) the effects of the spin-dependent scattering from impurities on the electrical transport were calculated,[9] and an unrealistically large GMR was found. Several reasons have been advanced; among them are a lack of knowledge of the type of defects, or the details thereof, which produce spin-dependent scattering, and the short circuit produced by the near matching of the defect and host potentials for one of the spin directions.[10] In a previous study of the resistivity of bulk Permalloy based on the spin-polarized relativistic KKR method,[11] it was found that relativistic corrections, although they may be quite small, were sufficient to avoid the near short circuits that appear due to the lack of scattering in the majority-spin channel when one performs a calculation in the so-called ''two current model'' in which the scattering for each direction of spin is treated independently. Therefore, while relativistic effects may be small for, e.g., cohesive properties of $3d$ transition metals, they are important to obtain realistic resistivities for ferromagnetic alloys.

Here we describe results of such calculations based on the spin-polarized relativistic screened KKR method for layered systems which uses the Kubo-Greenwood equation for the conductivity and the single site coherent-potential approximation (CPA) to incorporate the effect of impurities on electrical transport.[12,13] In this formalism the electrical conductivity for layered systems, i.e., systems which have only two-dimensional translational symmetry, is of the form

$$\sigma_{\mu\mu}(L)=\sum_{p,q=1}^{L}\sigma_{\mu\mu}^{pq}, \tag{1}$$

where $\sigma_{\mu\mu}^{pq}$ is the conductivity that describes the current in layer $p$ caused by an electric field in layer $q$,

$$\sigma_{\mu\mu}^{pq}=\frac{\hbar}{\pi N_0\Omega_{\mathrm{at}}}\mathrm{Tr}\langle J_\mu^p\,\mathrm{Im}\,G^+(\epsilon_F)J_\mu^q\,\mathrm{Im}\,G^+(\epsilon_F)\rangle. \tag{2}$$

In these equations $\mu\in\{x,y,z\}$, $L$ is the number of layers considered, $N_0$ is the number of atoms per plane of atoms, $\Omega_{\mathrm{at}}$ is the atomic volume, $\langle\cdots\rangle$ denotes an average over configurations, $J_\mu^p$ is the $\mu$th component of the current operator referenced to the $p$th plane, and $G^+$ is the electron propagator (one-particle Green's function) from plane $p$ to $q$ at the Fermi energy $\epsilon_F$. When we apply Eqs. (1) and (2) to calculate the resistivity of finite but otherwise perfect sys-

 

tems there are no corrections to Eq. (2); however, when we introduce impurities there are putative vertex corrections to the impurity-averaged propagators that we neglect.[14] For a detailed discussion of Eqs. (1) and (2) and the method applied see Ref. 13.

As our method is for semi-infinite systems (most previous *ab initio* calculations were for three-dimensional infinite periodic structures) a resistance arises in our calculations that is not present for periodic structures.[15] Even when semi-infinite systems are free of defects they exhibit a resistance because there is no translational invariance (periodicity) along the surface normal due to the finiteness of the system. All finite conductors have self-energy terms in their propagators $G^+$ (Green's functions) which describe their contact with leads or reservoirs. This resistance is proportional to the imaginary part of this self-energy which reflects the fact that an electron in an isolated conductor will eventually leak out into the leads attached to it.[15,16]

Here we calculate the resistivity and GMR of several model structures for currents in the plane of the layers (CIP).[17] In this foray we have limited ourselves to self-consistently calculating up to about 45 monolayers; therefore the structures are smaller than those studied experimentally. The resistance of these small structures depends on the boundary conditions imposed. To establish a well-defined Fermi level we place the structures whose resistance we calculate in contact with semi-infinite metals. This has the effect that information of the electron's momentum is lost when it leaves the system under consideration and goes into the semi-infinite metal, and thereby produces resistance. Had we used other boundary conditions, e.g., bounding the surfaces of the structure with reflecting walls, we would find no resistance if the structure is finite but otherwise perfect (pure). In the following sections we describe the effects on CIP resistivity and MR of such factors as size, layering, repetition of layering (superstructure), substrate, cap, alloying, and interdiffusion.

## II. COMPUTATIONAL DETAILS

All calculations reported here are based on the fully relativistic, spin-polarized screened Korringa-Kohn-Rostoker (KKR) method[18] for layered systems[12] for generating the corresponding self-consistent scattering potentials, whereby all interlayer distances refer to an fcc ''parent lattice''[19] corresponding to the experimental lattice spacing of the substrate (Cu : $a_0=6.8309$ a.u.; Pt : $a_0=7.4137$ a.u.; no surface or interface relaxations). For each system under consideration we have chosen the magnetization to be *uniformly* perpendicular to the planes of atoms. The electronic structure is calculated self-consistently using $45\mathbf{k}_\parallel$ points in the irreducible wedge of the surface Brillouin zone (ISBZ), the local-density functional described by Vosko *et al.*,[20] and we limited ourselves to scattering up to and including the $l=2$ channel (see Ref. 21). All calculations refering to interdiffused or alloyed systems are based on the coherent-potential approximation as described by Weinberger *et al.*[13] For the evaluation of the electrical conductivity tensor $1830\mathbf{k}_\parallel$ points in the ISBZ are used.

## III. APPLICATIONS

### A. Pure metals and statistically disordered alloys

We start by studying familiar problems such as the resistivity of finite pure metals and homogeneous statistically disordered alloys. In viewing Eq. (1), it is quite clear that for $L=n$ becoming very large,[22] say $n_0$, the resistivity for a pure metal approaches its bulk value, i.e., for a parent fcc lattice, $\rho_{xx}=\rho_{yy}=\rho_{zz}=0$, whereas for a statistically disordered (binary) alloy the so-called residual resistivity should be obtained, i.e., for a parent fcc lattice the nonvanishing diagonal elements of the resistivity tensor tend to a constant ($C$). In other words

$$\lim_{n\to n_0}\rho_{\mu\mu}(n)=\lim_{n\to n_0}\rho_{zz}(n)=\begin{cases}0 & ; \text{ pure metal}\\ C & ; \text{ statistically disordered alloy}\end{cases} \tag{3}$$

where $\mu=x$ or $y$. In Fig. 1(a) we show the CIP resistivity $\rho_{xx}(n)=\sigma_{xx}^{-1}(n)$ for three different structures $B_n$ sandwiched between two semi-infinite substrates of copper

$$\mathrm{Cu}(100)/B_n/\mathrm{Cu}(100). \tag{4}$$

Here $B_n$ is $n$ (two-dimensional translationally invariant) monolayers (ML) of (a) Cu, (b) Co, or (c) the statistically disordered binary alloy $Cu_{0.85}Co_{0.15}$. As one can see from this figure, all three curves show a $(1/n)$-like decay, whereby $n\rho_{xx}(n)$ becomes strictly linear in $n$ for $n\geqslant 30$; the slope of this function determines the value of $\rho_{xx}(n)$ for $n\to n_0$. This is illustrated in Figs. 1(b) and 1(c) for cases (a) and (c) together with the linear regression coefficients. From Figs. 1(a) and 1(b) it is evident that for a pure metal $\rho_{xx}(n)$ tends to zero as $n\to n_0$, while for the alloy a residual resistivity of about 2.2 $\mu\Omega$ cm is predicted. For small $n$ we note deviations from the linear behavior of $n\rho_{xx}(n)$ caused by the extremely small number of monolayers in $B_n$.

We have estimated the resistivity arising from a finite number of repeats of an atomic potential;[23] by using free-electron parameters appropriate for copper we find $\rho=39.7/n$ $\mu\Omega$ cm in the limit where the number of monolayers $n$ is large. This estimate for $n\rho_{xx}(n)$ of 39.7 $\mu\Omega$ cm compares rather well with the 28.9 $\mu\Omega$ cm we found from the linear regression, see Fig. 1(b). To show that this resistivity comes from the boundary conditions we unwittingly introduce when we embed the copper layers in which we are interested in a copper matrix (which acts as a reservoir) we have considered $\mathrm{Cu}(100)/\mathrm{Vac}_m/\mathrm{Cu}_n/\mathrm{Vac}_\infty$, where Vac denotes an empty layer, which mimics a free-standing slab of a finite number of Cu layers. For $n=6$ and $m=3$ the resistivity drops from 3.26 $\mu\Omega$ cm for $Cu_6$ embedded by Cu(100) to 0.01 $\mu\Omega$ cm; this value is close enough to zero to confirm that the resistivity for a perfectly flat film of a metal is indeed zero.

For pure cobalt we find a similar variation albeit with a somewhat higher resistivity. By embedding cobalt in copper we produce an additional resistance, beyond that coming from the finite number of repeats, that comes from the charge

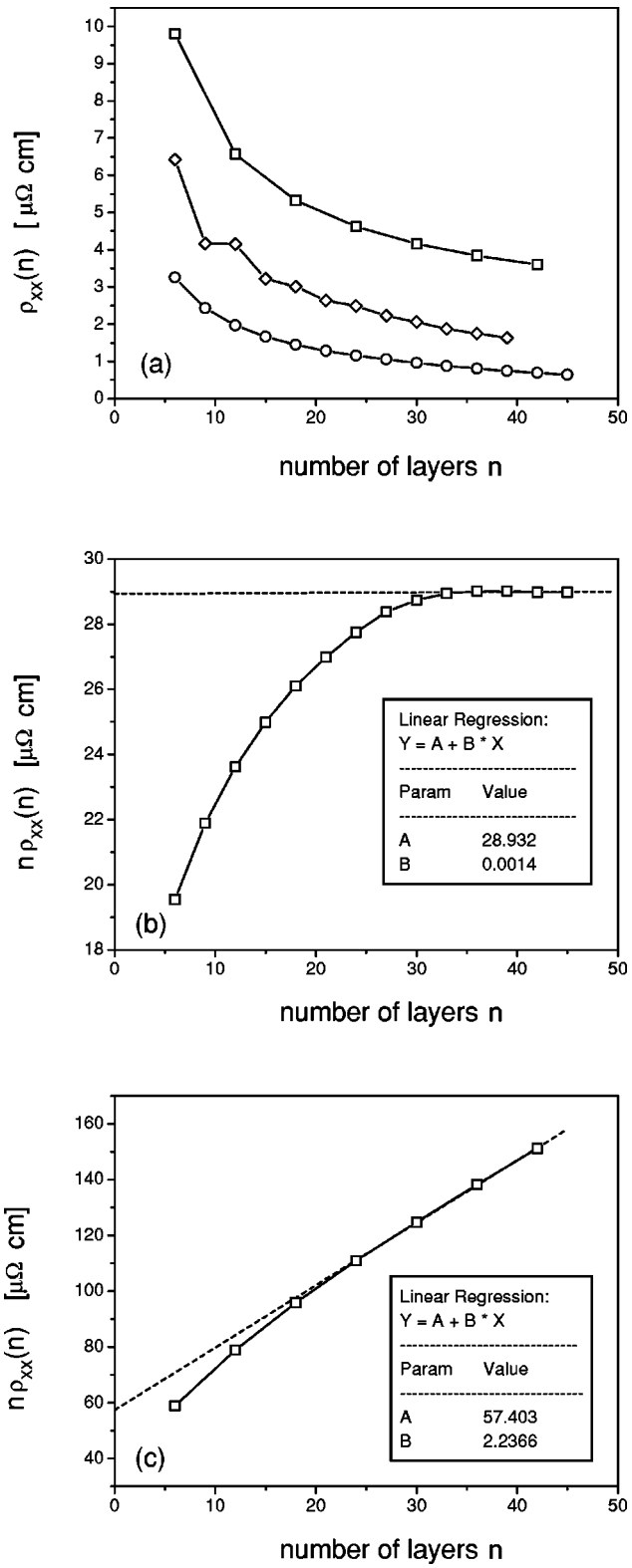


FIG. 1. (a) CIP resistivity $\rho_{xx}(n)$ of a slab consisting of $n$ monolayers of Cu (circles), Co (diamonds), and the statistically disordered homogeneous alloy $Cu_{0.85}Co_{0.15}$ (squares) embedded in fcc Cu(100). (b) $n\rho_{xx}(n)$ for $n$ monolayers of Cu (squares), together with the linear fit (dashed line) of $n\rho_{xx}(n)$ for $n \geqslant 30$ with respect to $n$. (c) $n\rho_{xx}(n)$ for $n$ monolayers of the statistically disordered homogeneous alloy $Cu_{0.85}Co_{0.15}$ (squares), together with the linear fit (dashed line) of $n\rho_{xx}(n)$ for $n \geqslant 25$ with respect to $n$. In the insets to (b) and (c) $A$ and $B$ refer to the fitting coefficients.

redistribution at the interfaces of the cobalt with the copper caused by the mismatch in potentials of the dissimilar metals.

The calculated resistivity for $Cu_{0.85}Co_{0.15}$ of about 2.2 $\mu\Omega$ cm as $n \to n_0$ is low in comparison with the (experimental) bulk residual resistivity per atomic percent Co, which for dilute Co ($<1\%$) is about 6 $\mu\Omega$ cm at%.[24] It should be recalled, however, that in a semi-infinite system such as in cases (b) and (c) the Fermi energy of the system is that of the substrate, i.e., that of fcc Cu in the present case. The quoted residual resistivity for $Cu_{0.85}Co_{0.15}$ refers to the Fermi energy of fcc Cu and not to that of the statistically disordered fcc bulk alloy $Cu_{0.85}Co_{0.15}$. Therefore, a proper comparison to the (experimental) bulk residual resistivity of $Cu_{0.85}Co_{0.15}$ implies substrates of the same composition.

### B. Repetitions and superstructures

Very often magnetic multilayers consist of repeating a pattern of layers (motif), i.e., semi-infinite systems of the type

$$\text{Substrate}/(B_n)_N/A_p \tag{5}$$

are considered, where the substrate is of a particular surface orientation, $B_n$ refers to a repetition unit (motif) of $n$ layers that is repeated $N$ times, and $A_p$ to a finite ($p$ monolayers) or semi-infinite ($p \to \infty$) cap of an appropriate metal or vacuum. The total number $L$ of atomic layers (actual thickness of the magnetic multilayer system) to be summed over in Eq. (1) is then in principle given by $L = Nn + p$. In this case one has to expect that for a sufficiently large number of repetitions, say $N_0$, the resistivity and MR approaches its asymptotic or saturation value. By choosing Pt(100) as substrate and a free surface as a cap we calculated the resistivity and MR of multilayers consisting of $N$ repeats of CoPt (i.e., $B_{n=2}$, $A_{p=0}$, hence omitting the cap dependence $p$ in the following)

$$\text{Pt}(100)/(\text{CoPt})_N \tag{6}$$

corresponding to ferromagnetic (p, parallel) and antiferromagnetic (ap, antiparallel) alignments of the magnetizations of adjacent Co slabs. As the magnetization of a ML of Co is perpendicular to the plane of the layer, these designations imply that in the p configuration they all point in the same direction and perpendicular to the planes of Co atoms, whereas they alternate in direction with respect to the normal to the layers in the ap configuration.

Denoting the magnetic configuration of the multilayer with a superscript $\alpha$ (p or ap) for a large enough number of repetitions the resistivity reaches its asymptotic value

$$\lim_{N \to N_0} \rho^{\alpha}_{\mu\mu}(n;N) = C^{\alpha}(n), \tag{7}$$

where $\mu = x,y$. We define the MR ratio $\eta_{xx}(n;N)$ as

$$\eta_{xx}(n;N) = \frac{\rho^{\text{ap}}_{xx}(n;N) - \rho^{\text{p}}_{xx}(n;N)}{\rho^{\text{ap}}_{xx}(n;N)}; \tag{8}$$

this approaches a saturation value of

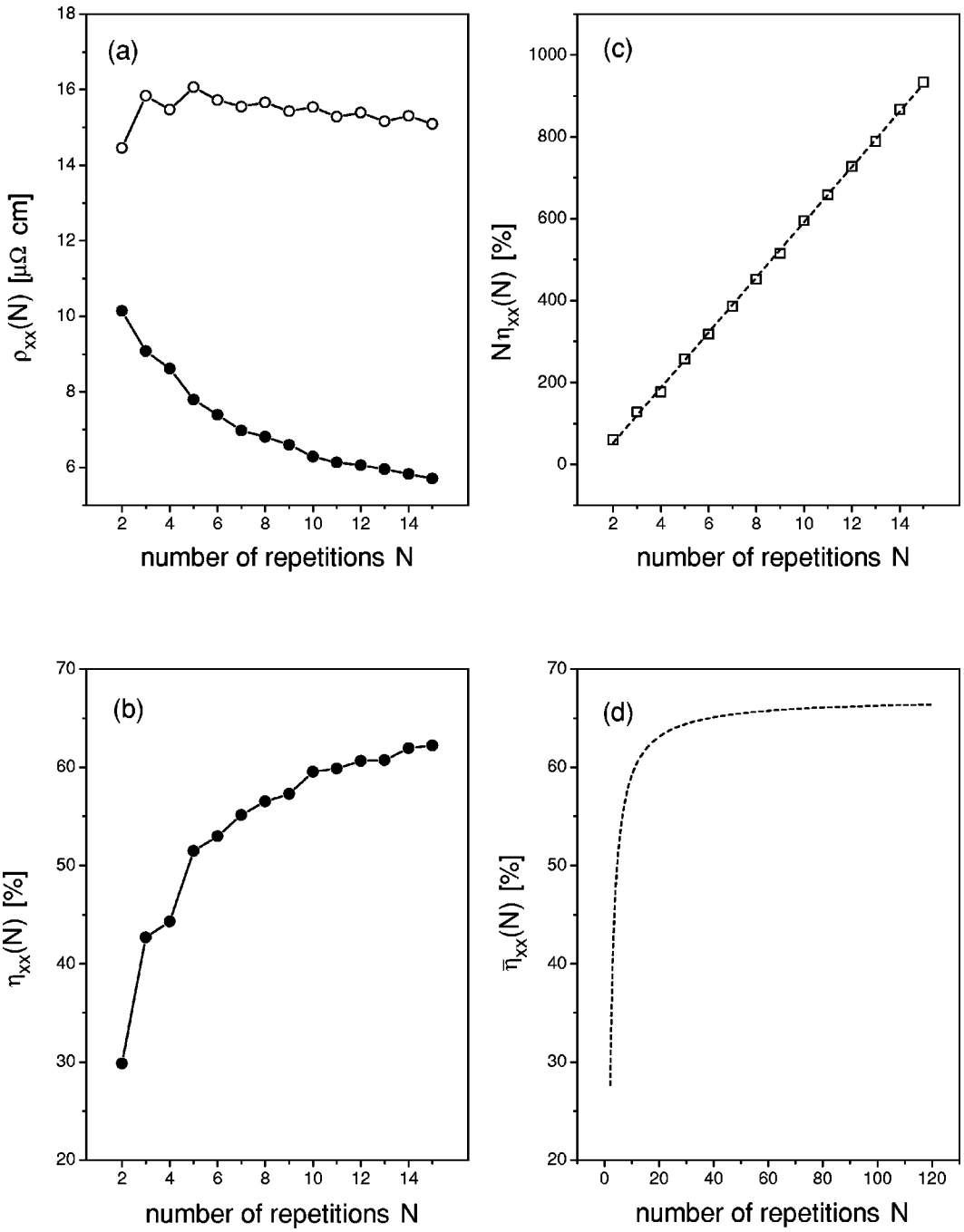


FIG. 2. (a) Parallel (full circles) and antiparallel (open circles) CIP resistivities $\rho_{xx}^{\alpha}(N)$, (b) CIP-MR $\eta_{xx}(N)$, and (c) $N\eta_{xx}(N)$ of a multilayer consisting of $N$ repetitions of CoPt on top of Pt(100). The extrapolated CIP-MR $\overline{\eta}_{xx}(N)$ in (d) is based on the linear fit of $N\eta_{xx}(N)$ with respect to $N$ shown as the dashed line in (c).

$$\lim_{N\to N_0} \eta_{xx}(n;N) = 1 - \frac{C^{\mathrm{p}}(n)}{C^{\mathrm{ap}}(n)}. \tag{9}$$

In Fig. 2 the CIP resistivity $\rho_{xx}^{\alpha}(n;N)$, CIP-MR $\eta_{xx}(n;N)$, and $N\eta_{xx}(n;N)$ are displayed for Pt(100)/$(\mathrm{CoPt})_N$ as a function of the number of repetitions $N$. Based on the linear fit for $N\eta_{xx}(n;N)$, see Fig. 2(c), the fitted CIP-MR ratios $\overline{\eta}_{xx}(n;N)$ are shown in Fig. 2(d) in such a manner that the saturation value can be easily read off. As can be seen from the figures, $\rho_{xx}^{\mathrm{p}}(n;N)$ and $\rho_{xx}^{\mathrm{ap}}(n;N)$, as well as $\eta_{xx}(n;N)$, show oscillations with a period of two, clearly causing some deviations from the linear behavior of $N\eta_{xx}(n;N)$ with respect to $N$. As there are no impurities the electronic structure controls the resistivity and MR of these finite multilayers. In this case it is not surprising to find oscillations inasmuch as the corresponding interlayer exchange coupling energy shows oscillations with respect to the number of repetitions in this type of system.[25] These oscillations are related to the alternation of even and odd numbers of repetitions. When $N$ is odd there is a net magnetization for the multilayer in the ap configuration, and the MR is expected to be less than what it would be if one achieved zero magnetization; for even $N$ one always has zero magnetization for the ap state. Figure 2(d) shows

that for a small number of repetitions, the corresponding value for the GMR can be far off the saturation value, and that for $N \geqslant 50$ very little is gained by further repetitions.

Quite clearly in this particular example, the repeated unit is rather small ($n=2$) as it consists of one layer of Co and one layer Pt; however, it illustrates that there is convergence to an asymptotic or saturation value in the resistivities and GMR. In this context we recall that a superstructure, such as alternating layers of Co and Pt on Pt(100), is not a superlattice, although for practical purposes in many cases the saturation value for the GMR virtually coincides with that obtained from a genuine superlattice calculation, i.e., from a calculation for a system with three-dimensional translational invariance (three-dimensional periodic boundary conditions). For example, for the system $Cu(100)/(Cu_3Ni_3)_N/Cu(100)$ we predicted a saturation value for the CIP-MR of about 25%,[26] while a nonrelativistic supercell calculation for $Cu_3Ni_3(100)$ yielded about 23%.[27]

The present example of a CoPt superstructure on Pt(100) serves as another illustration for the dependence of the resistivity on the boundary conditions. In these calculations one surface was free (no cap), since the ''right'' semi-infinite system refered to vacuum, and we can compare these resistivities to those when the vacuum is replaced by a semi-infinite cap of Pt. Therefore, we have recalculated for a few cases the CIP resistivities $\rho^{\alpha}_{xx}(n;N)$ and the corresponding GMR of $Pt(100)/(CoPt_N/Pt(100)$, and compared them with those when one surface is free. As one can see from Fig. 3(a) for free surfaces the parallel as well as the antiparallel CIP resistivity is substantially smaller than the corresponding value in the case of a semi-infinite Pt cap. It is clear that the cap is a reservoir which acts as a source of resistance; as the number of repetitions increases these differences become increasingly smaller because the effects of the boundary are diminished.

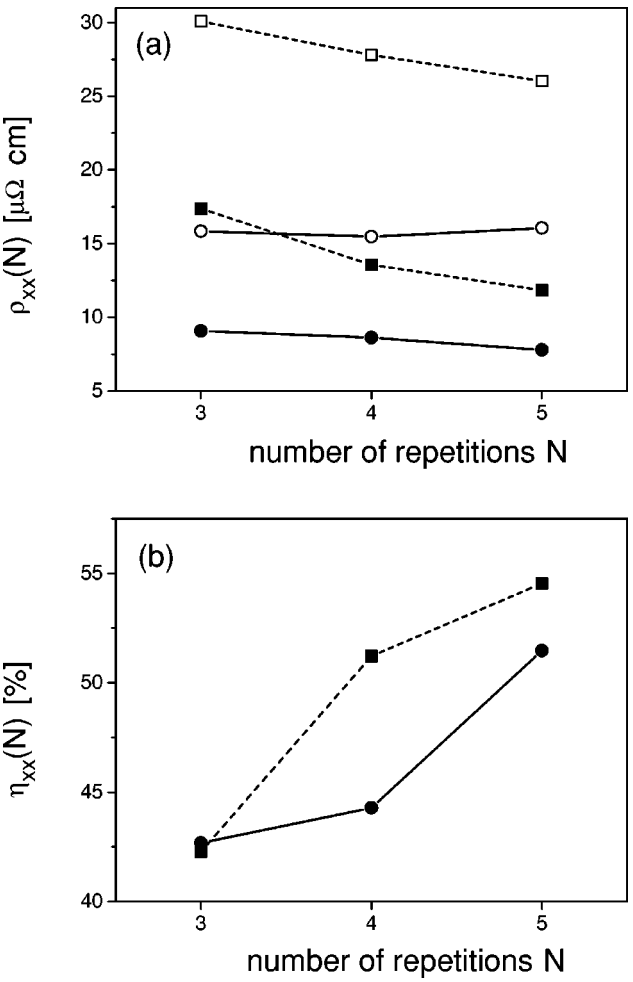


FIG. 3. (a) Parallel (full symbols) and antiparallel (open symbols) CIP resistivities $\rho^{\alpha}_{xx}(N)$ and (b) CIP-MR $\eta_{xx}(N)$ of a multilayer consisting of $N$ repetitions of CoPt on top of Pt(100). Squares refer to a semi-infinite Pt cap; circles refer to free surfaces.

### C. Trilayer systems

One variant of the spin-valve structure is

$$Cu(100)/B_nCu_mB_n/Cu(100), \tag{10}$$

where $B_n$ is a magnetic slab of thickness $n$. For a sufficiently large number of Cu-spacer layers ($m_0$) and for any magnetic configuration $\alpha$ of the magnetic slabs

$$\lim_{m\to m_0} \rho^{\alpha}_{\mu\mu}(m;n)=0 \tag{11}$$

as the CIP is short-circuited through the Cu layers. We consider the slab $B_n$ to be interdiffused over two ML at the Co/Cu interfaces,

$$B_n=\begin{pmatrix} Cu_{1-c}Co_c \\ Cu_cCo_{1-c} \\ Co \\ \vdots \\ Co \\ Cu_cCo_{1-c} \\ Cu_{1-c}Co_c \end{pmatrix}. \tag{12}$$

In Figs. 4(a) and 4(b) we show $\rho^{\alpha}_{xx}(m;n)$ and the corresponding $\eta_{xx}(m;n)$ with respect to the thickness $m$ of the Cu spacer for $n=3$,

$$B_3=\begin{pmatrix} Cu_{1-c}Co_c \\ Cu_{2c}Co_{1-2c} \\ Cu_{1-c}Co_c \end{pmatrix}, \tag{13}$$

for two concentrations of interdiffusion, $c=0$ and $c=0.05$. As can be seen from Fig. 4(a) the resistivities $\rho^{\alpha}_{xx}(m;n=3)$ show a $(1/m)$-like decay; the same holds true for the corresponding CIP-MR in Fig. 4(b) for small values of $m$ ($m \leqslant 6$). We note that the GMR is considerably enhanced by interdiffusion. The increase in MR ratio due to interdiffusion comes from the large increase in the difference between the resistivities for parallel and antiparallel configurations (in the numerator); this comes more from the increase of $\rho^{ap}$ than $\rho^{p}$. By adding additional layers of copper, $m \geqslant 1$, we dilute the effect of scattering from interdiffusion which is confined to the cobalt and neighboring layers of copper; this dilution causes the resistivities to decay as $1/m$ as one can see from this figure.[28] The more rapid decrease in the GMR comes from the *additional* effect of the exponential decay of the

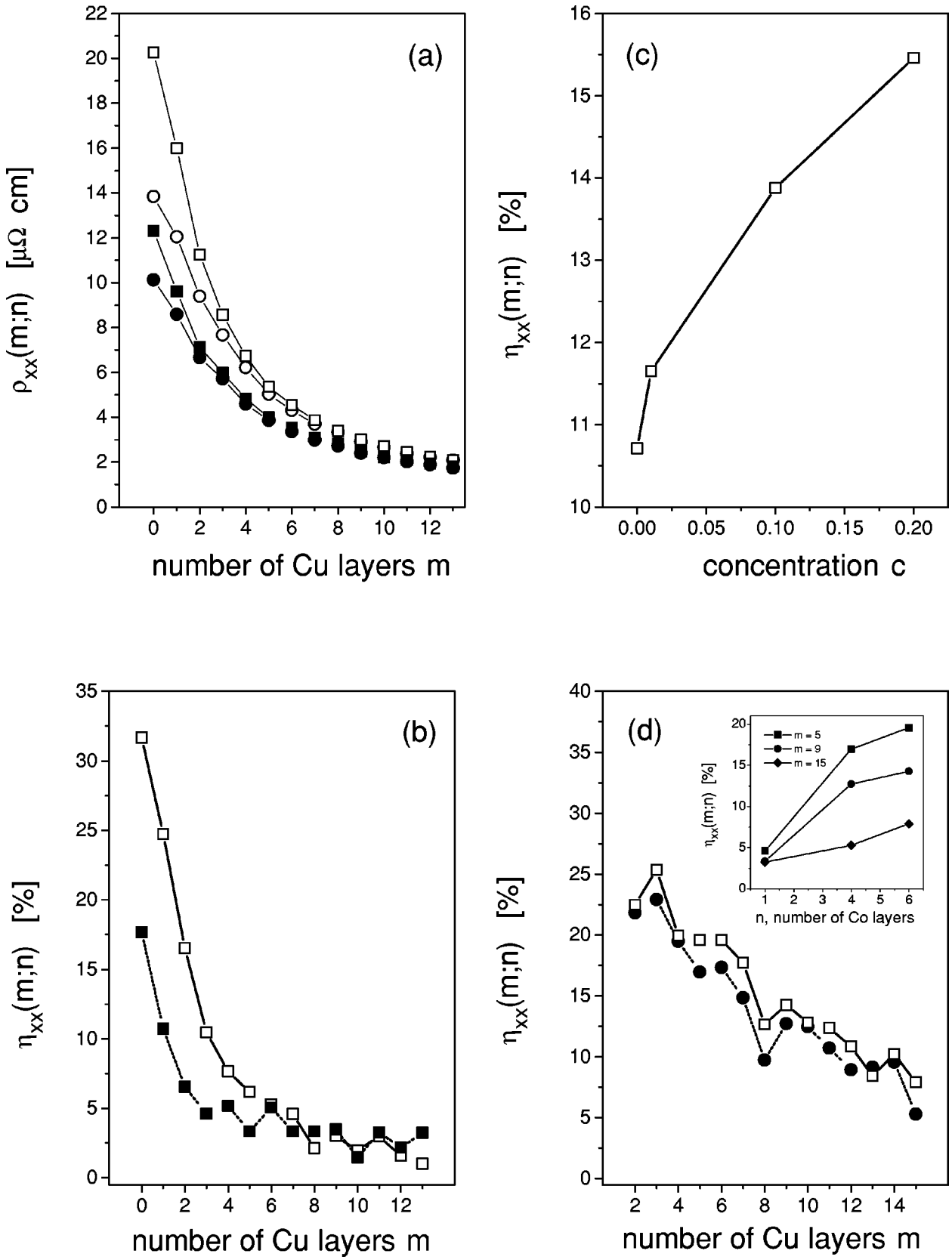


FIG. 4. Trilayer system $B_nCu_mB_n$ embedded in fcc Cu(100) with $B_n$ denoting a Co slab together with its interdiffused Co/Cu interfaces (see text): (a) Parallel (circles) and antiparallel (squares) CIP resistivities $\rho^{\alpha}_{xx}(m;n)$ for $n=3$. Full symbols refer to no interdiffusion, open symbols to 5% interdiffusion at the Co/Cu interfaces. (b) CIP-MR $\eta_{xx}(m;n)$ for $n=3$. Full symbols refer to no interdiffusion, open symbols to 5% interdiffusion at the Co/Cu interfaces. (c) Interdiffusion concentration dependence of the CIP-MR $\eta_{xx}(m;n)$ for $n=6$ and $m=9$. (d) CIP-MR $\eta_{xx}(m;n)$ of pure Co layers ($B_n=Co_n$) for $n=4$ (filled circles) and $n=6$ (open squares). The inset shows $\eta_{xx}(m;n)$ for $n=1$, 4, and 6 monolayers of Co separated by $m=5$ (squares), 9 (circles), and 15 (diamonds) monolayers of Cu.

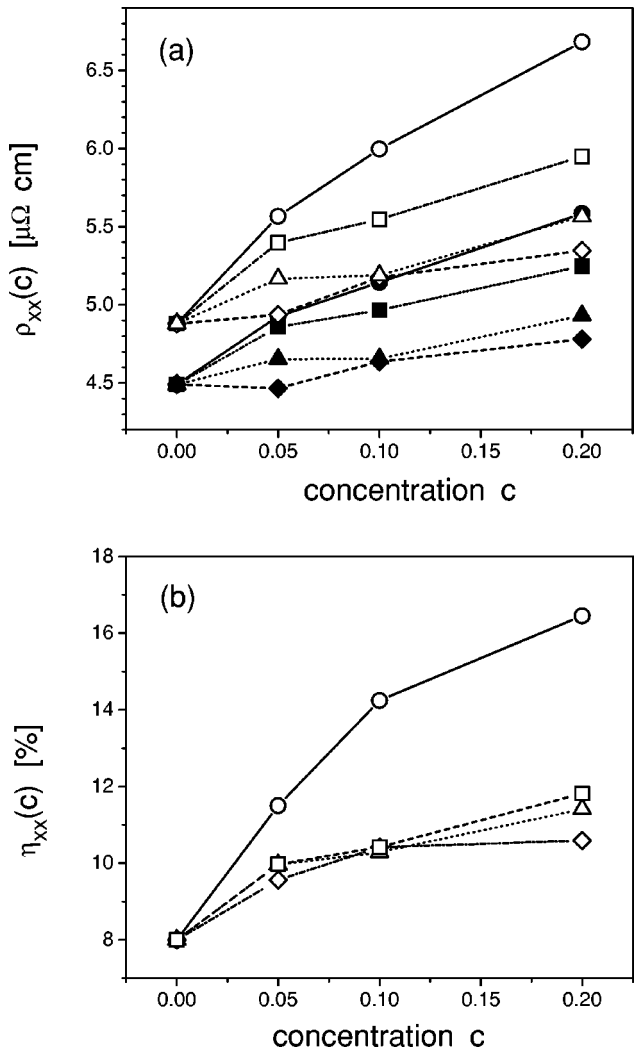


FIG. 5. Effect of interdiffusion and homogeneous alloying on (a) the CIP resistivities $\rho^{\alpha}_{xx}(c)$, $\alpha=$p,ap, and (b) the CIP-MR $\eta_{xx}(c)$ in the multilayer system $Co_9Cu_7Co_9$ embedded in fcc Cu(100) as a function of the concentration. Circles refer to interdiffusion at the Co/Cu interfaces; diamonds, triangles, and squares to homogeneous alloying in the Co layers with Fe, Ni, and Cu, respectively. Full symbols correspond to the parallel configuration, open symbols to the antiparallel configuration.

CIP-MR as we increase the distance between scattering planes.[29] For $m \geqslant 6$, $\rho^{\mathrm{ap}}$, and $\rho^{\mathrm{p}}$ are very close in value, therefore the calculated GMR in this regime of spacer layers can be determined only up to an error of about 1%. The GMR enhancement due to interdiffusion is shown in more detail for $n=6$ and $m=9$ in Fig. 4(c),

$$B_6=\begin{pmatrix} \mathrm{Cu}_{1-c}\mathrm{Co}_c \\ \mathrm{Cu}_c\mathrm{Co}_{1-c} \\ \mathrm{Co} \\ \mathrm{Co} \\ \mathrm{Cu}_c\mathrm{Co}_{1-c} \\ \mathrm{Cu}_{1-c}\mathrm{Co}_c \end{pmatrix}, \tag{14}$$

for $c$ varying between 0 and 20%.

To determine the GMR due to solely the dependence of the electronic structure on the magnetic configuration of the multilayer we show in Fig. 4(d) $\eta_{xx}(m;n)$ for $n$ ML of pure Co

$$B_n=\mathrm{Co}_n, \quad n=4,6, \tag{15}$$

as a function of the thickness of the Cu spacer $m$. In particular this figure demonstrates [in comparison with Fig. 4(b)] that the actual value of $\eta_{xx}(m;n)$ is governed by the thickness of the magnetic slabs. However, as we show in the inset for $m=5$, 9, and 15, the increase in $\eta_{xx}(m;n)$ in going from four to six ML of Co is much less than increasing $n$ from one to four. For two monolayers of Co separated by 2 ML of Cu, i.e., $CuCoCu_2CoCu$, we find a CIP-MR ratio of 17.7%; this compares very favorably with the 23% found by Schep *et al.* for the superlattice $Co_2Cu_2$.[3] We do not quote resistivities as they are not comparable; our finite system $CuCoCu_2CoCu$ is embedded in semi-infinite Cu while theirs is for a $Co_2Cu_2$ superlattice. For two slabs of Co each of 4 ML thickness and separated by 4 ML of Cu we find a CIP-MR ratio of 19.5% which is higher than the 5% found by Schep *et al.* for $Co_4Cu_4$.[3]

### D. Interdiffusion, alloying, and repetitions

A more generic form of a magnetic multilayer is

$$\mathrm{Substrate}/(B_{n_1}S_{m_1}B_{n_2}S_{m_2})_N/A_p, \tag{16}$$

where the $B_{n_i}$ are magnetic slabs, the $S_{m_i}$ nonmagnetic spacers, and $A_p$ refers to a finite ($p$ ML) or semi-infinite ($p \rightarrow \infty$) cap. The thickness $L$ (in ML) of such a multilayer to be summed over in Eq. (1) is, in principle, given by $L=N(n_1+m_1+n_2+m_2)+p$. In principle, the resistivity $\rho^{\alpha}_{\mu\mu}$ depends on all parameters determining the thickness $L$,

$$\rho^{\alpha}_{\mu\mu} \equiv \rho^{\alpha}_{\mu\mu}(n_1;m_1;n_2;m_2;N;p), \tag{17}$$

as well as on the composition of the various layers. In the following we will stay in the limit where $m_i \ll m_0$ and $n_i \ll n_0$, so that we retain a finite number of ML in each slab and stay away from bulk values of the resistivities of the constituent layers.

To elucidate the different effects on the resistivity of interdiffusion between layers and homogeneous alloying within the magnetic layers, we have chosen to generalize a system studied previously in terms of a supercell approach, namely $Co_9Cu_7$.[5] The setup for the present study refers to the following multilayer structure:

$$\mathrm{Cu}(100)/B_{11}\mathrm{Cu}_5B_{11}/\mathrm{Cu}(100), \tag{18}$$

where

$$B_{11}=\begin{pmatrix} \mathrm{Cu}_{1-c}\mathrm{Co}_c \\ \mathrm{Cu}_c\mathrm{Co}_{1-c} \\ \mathrm{Co} \\ \mathrm{Co} \\ \mathrm{Co} \\ \mathrm{Co} \\ \mathrm{Co} \\ \mathrm{Co} \\ \mathrm{Co} \\ \mathrm{Cu}_c\mathrm{Co}_{1-c} \\ \mathrm{Cu}_{1-c}\mathrm{Co}_c \end{pmatrix} \quad \text{or} \quad \begin{pmatrix} \mathrm{Cu} \\ \mathrm{Co}_{1-c}X_c \\ \mathrm{Co}_{1-c}X_c \\ \mathrm{Co}_{1-c}X_c \\ \mathrm{Co}_{1-c}X_c \\ \mathrm{Co}_{1-c}X_c \\ \mathrm{Co}_{1-c}X_c \\ \mathrm{Co}_{1-c}X_c \\ \mathrm{Co}_{1-c}X_c \\ \mathrm{Co}_{1-c}X_c \\ \mathrm{Cu} \end{pmatrix}, \qquad (19)$$

and $X=\mathrm{Fe,Ni,Cu}$. The first column corresponds to a Co slab with interdiffusion at the Co/Cu interfaces; the second describes the influence of homogeneous alloying in the Co layers with no interdiffusion at the interfaces. As can be seen from Fig. 5, which contains the CIP resistivities $\rho^{\alpha}_{xx} \equiv \rho^{\alpha}_{xx}(c)$, $\alpha=\mathrm{p}$, ap, and CIP-MR ratios $\eta_{xx} \equiv \eta_{xx}(c)$ for all these cases, homogeneous alloying of the Co slabs increases $\eta_{xx}(c)$ only moderately, the increase itself being almost independent of the alloying element. On the other hand, interdiffusion at the interfaces has a much larger effect; compared with no interdiffusion ($c=0$) the GMR $\eta_{xx}(c)$ is doubled for a 20% interdiffusion ($c=0.2$). By looking ahead at the results shown in Fig. 6, we can anticipate that the curves of the GMR in Fig. 5(b) for the Co layers alloyed with Fe or Ni will reach a maximum or plateau and will then eventually drop to the GMR value corresponding to pure Fe or Ni slabs. At the cobalt rich end, we can compare our value of the CIP-MR of 8% for $\mathrm{Co_9Cu_7Co_9}$ with the 30% found from the supercell approach for $\mathrm{Co_9Cu_7}$;[5] as we found from our previous study on $(\mathrm{Cu_3Ni_3})_N$,[26] this smaller value comes from our not repeating the motif $\mathrm{Co_9Cu_7}$ a sufficient number of times so as to mimic the periodic repetition present in the supercell calculation.

To study the interplay of repetitions and alloying we considered

$$\mathrm{Cu}(100)/(B_3\mathrm{Cu}_3)_5/\mathrm{Cu}(100), \qquad (20)$$

where

$$B_3=\begin{pmatrix} \mathrm{Fe}_c\mathrm{Co}_{1-c} \\ \mathrm{Fe}_c\mathrm{Co}_{1-c} \\ \mathrm{Fe}_c\mathrm{Co}_{1-c} \end{pmatrix}, \quad 0\leqslant c\leqslant 1. \qquad (21)$$

In Figs. 6(a) and 6(b) the CIP resistivities $\rho^{\alpha}_{xx}(c)$ and corresponding MR $\eta_{xx}(c)$ of this system are shown with respect to the Fe concentration. As can be seen from Fig. 6(b) $\eta_{xx}(c)$ increases substantially with increasing Fe concentration up to about 30% of Fe, then it varies only slightly till beyond 90% of Fe, at which point it drops sharply to the value for pure Fe layers. It is interesting to note from Fig. 6(a) that changes of the MR $\eta_{xx}(c)$ with respect to the Fe concentration are mainly caused by $\rho^{\mathrm{ap}}_{xx}(c)$, which for $c \leqslant 0.3$ increases considerably more rapidly than $\rho^{\mathrm{p}}_{xx}(c)$. With respect to concentration both resistivities, $\rho^{\mathrm{p}}_{xx}(c)$ and $\rho^{\mathrm{ap}}_{xx}(c)$, show shapes that are typically seen in bulk magnetic alloy systems,[11] i.e., the maxima in the resistivities do not necessarily coincide with $c=0.5$, although the maximum in the corresponding MR $\eta_{xx}(c)$ does; see Figs. 6(a) and 6(b).

In contrast to the previous case where we considered the effects of alloying, we consider a final example of the effects of interdiffusion and repetition in the following multilayer system:

$$\mathrm{Cu}(100)/(B_5\mathrm{Cu})_5/\mathrm{Cu}(100), \qquad (22)$$

$$B_5=\begin{pmatrix} \mathrm{Cu}_{1-c}\mathrm{Co}_c \\ \mathrm{Cu}_c\mathrm{Co}_{1-c} \\ \mathrm{Co} \\ \mathrm{Cu}_c\mathrm{Co}_{1-c} \\ \mathrm{Cu}_{1-c}\mathrm{Co}_c \end{pmatrix}. \qquad (23)$$

In Figs. 6(c) and 6(d) $\rho^{\mathrm{p}}_{xx}(c)$ and $\rho^{\mathrm{ap}}_{xx}(c)$ and the corresponding $\eta_{xx}(c)$ are displayed as a function of the amount (concentration $c$) of interdiffusion. From these two figures it is evident that, for a multilayer with repetition, interdiffusion of only a few % increases the GMR quite dramatically, since $\eta_{xx}(c)$ goes up to about 40% for a 10% interdiffusion, whereas it is only 17% for the same structure without interdiffusion.

## IV. SUMMARY AND CONCLUSION

We have used the spin-polarized relativistic screened KKR method for layered systems together with the CPA to calculate electrical transport properties of magnetic multilayers within the Kubo-Greenwood formalism. We show that one can calculate the resistivity and GMR of model structures with *no* adjustable parameters other than the lattice constant, i.e., in an *ab initio* manner. Our method determines contributions to the GMR of multilayer systems coming from both electronic structure and spin-dependent scattering off impurities. In this foray we have limited ourselves to CIP and to self-consistently calculating up to about 45 monolayers; therefore the structures are smaller than those studied experimentally. The resistance of these small structures depends on the boundary conditions imposed. To establish a well-defined Fermi level we placed them in contact with semi-infinite metals, and thereby produced resistance. When we used other boundary conditions, e.g., bounding one or both of the surfaces of the structure with vacuum, we find the resistance decreases. Indeed with both surfaces bounded by vacuum layers to simulate reflecting boundary conditions we find the resistance of a perfectly flat film of a pure metal goes to zero, as one expects.

We have described effects on CIP resistivity and MR due to such factors as: the finite size of and boundary conditions placed on the structure, the substrate and cap, the superstructure (repetition of a motif), and alloying in the magnetic

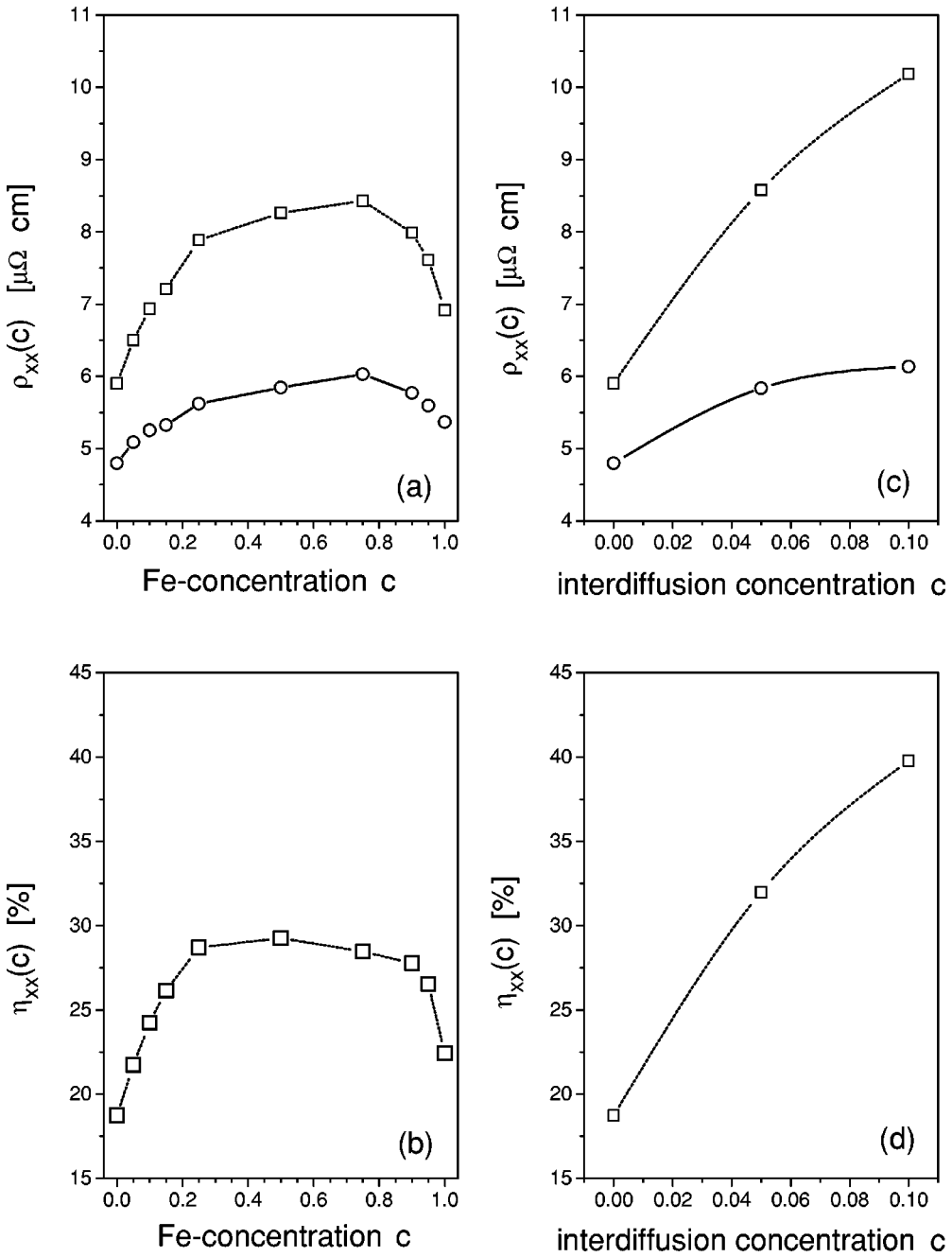


FIG. 6. Parallel (circles) and antiparallel (squares) CIP resistivities $\rho_{xx}^{\alpha}(c)$ and CIP-MR $\eta_{xx}(c)$ for the multilayer system $(Co_3Cu_3)_5$ embedded in fcc Cu(100) as a function of the concentration. (a) and (b) refer to homogeneous alloying in the Co layers with Fe; (c) and (d) to interdiffusion at the Co/Cu interfaces.

slabs and interdiffusion between layers. To elaborate and pin-point these effects we determined their dependence on: the number of layers $n$, the number of repetitions $N$ of the motif $(B_n)_N$, the thickness of the individual slabs, and the amount (concentration) of interdiffusion and alloying. Having in mind all these parameters one readily understands that (1) a comparison with experiment is only useful for well-characterized samples and (2) there are quite a few possibilities to optimize the GMR of magnetic multilayer systems. One salient result of our study is to confirm that spin-dependent scattering due to interdiffusion at interfaces has a far more pronounced effect on the CIP-MR than an equivalent amount of scattering arising from alloying the magnetic layers.

As we use a spin-polarized relativistic approach the dependence of the conductivity on the orientation of the magnetization relative to the layers can be determined without further parameters or approximations. These results,[30] as well as those for current perpendicular to the plane of the layers, will be presented elsewhere.

## ACKNOWLEDGMENTS

We would like to thank Ingrid Mertig, Albert Fert, and Walter Kohn for helpful discussions. This research was supported by the Austrian Science Foundation (P11626-PHY), the Center for Computational Materials Science in Vienna (GZ308.941), and we wish to thank the CNRS-IDRIS Com-

puter Center for calculations done on the T3E machine. The work by P.M.L. was supported by the Office of Naval Research (N00014-96-1-0203), together with the Defense Advanced Research Projects Agency (N00014-96-1-1207), the National Science Foundation (INT-9602192), and NATO (CRG 960340); he thanks Professor Albert Fert and the Laboratoire de Physique des Solides in Orsay, France, for their hospitality during his sabbatical stay there.

[1] P. M. Levy and S. Zhang, J. Magn. Magn. Mater. **151**, 315 (1995); **164**, 284 (1996).

[2] K. M. Schep, P. J. Kelly, and G. E. W. Bauer, Phys. Rev. Lett. **74**, 586 (1995).

[3] K. M. Schep, P. J. Kelly, and G. E. W. Bauer, Phys. Rev. B **57**, 8907 (1998).

[4] I. Mertig, R. Zeller, and P. H. Dederichs, Phys. Rev. B **47**, 16 178 (1993); I. Mertig, P. Zahn, M. Richter, H. Eschrig, R. Zeller, and P. H. Dederichs, J. Magn. Magn. Mater. **151**, 363 (1995); P. Zahn, I. Mertig, M. Richter, and H. Eschrig, Phys. Rev. Lett. **75**, 2996 (1995).

[5] P. Zahn, J. Binder, I. Mertig, R. Zeller, and P. H. Dederichs, Phys. Rev. Lett. **80**, 4309 (1998).

[6] T. Oguchi, J. Magn. Magn. Mater. **126**, 519 (1993); Mater. Sci. Eng., B **31**, 111 (1995).

[7] M. D. Stiles, J. Appl. Phys. **79**, 5805 (1996); W. H. Butler, X.-G. Zhang, D. M. C. Nicholson, T. C. Schulthess, and J. M. MacLaren, Phys. Rev. Lett. **76**, 3216 (1996); K. M. Schep, J. B. A. N. van Hoof, P. J. Kelly, G. E. W. Bauer, and J. E. Inglesfield, Phys. Rev. B **56**, 10 805 (1997).

[8] J. M. MacLaren, S. Crampin, D. D. Vvedensky, R. C. Albers, and J. B. Pendry, Comput. Phys. Commun. **60**, 365 (1990).

[9] W. H. Butler, J. M. MacLaren, and X.-G. Zhang, in *Magnetic Ultrathin Films, Multilayers and Surfaces/Interfaces and Characterization*, edited by B. T. Jonker, S. A. Chambers, R. F. C. Farrow, C. Chappert, R. Clarke, W. J. M. deJonge, T. Egami, P. Grünberg, K. M. Krishnan, E. E. Marinero, C. Rau, and S. Tsunashima, MRS Symposia Proceedings No. 313 (Materials Research Society, Pittsburgh, 1993), p. 59; R. K. Nesbet, J. Phys.: Condens. Matter **6**, L449 (1994); Int. J. Quantum Chem., Quantum Chem. Symp. **28**, 77 (1995).

[10] W. H. Butler (private communication).

[11] J. Banhart and H. Ebert, Europhys. Lett. **32**, 517 (1995); J. Banhart, A. Vernes, and H. Ebert, Solid State Commun. **98**, 129 (1996); H. Ebert, A. Vernes, and J. Banhart, *ibid.* **54**, 8479 (1996); J. Banhart, H. Ebert, and A. Vernes, Phys. Rev. B **56**, 10 165 (1997); J. Banhart, Philos. Mag. B **77**, 85 (1998); **77**, 105 (1998).

[12] L. Szunyogh, B. Újfalussy, and P. Weinberger, Phys. Rev. B **51**, 9552 (1995); **51**, 12 836 (1995).

[13] P. Weinberger, P. M. Levy, J. Banhart, L. Szunyogh, and B. Újfalussy, J. Phys.: Condens. Matter **8**, 7677 (1996).

[14] In considering the resistivity due to impurity scattering we have neglected vertex corrections due to our use of impurity averaged propagators in calculating the conductivity with the Kubo-Greenwood equation. This vanishes for CIP when one scatters *s* waves; for more realistic scattering this correction has been found to be small for bulk alloys, see Ref. 21.

[15] S. Datta, *Electronic Transport in Mesoscopic Systems* (Cambridge University Press, Cambridge, England, 1995), see in particular, pp. 151–155.

[16] For current in the plane of the layers (CIP) the contact or Sharvin resistance does not enter; however, for current perpendicular to the plane of the layers (CPP) it may contribute.

[17] While we determined the resistivity for current in and perpendicular to the plane of the layers (CIP/CPP), here we report only on our results for CIP.

[18] R. Zeller, P. H. Dederichs, B. Újfalussy, L. Szunyogh, and P. Weinberger, Phys. Rev. B **52**, 8807 (1995).

[19] P. Weinberger, Philos. Mag. B **77**, 509 (1997).

[20] S. Vosko, L. Wilk, and M. Nusair, Can. J. Phys. **58**, 1200 (1980).

[21] J. Banhart, H. Ebert, P. Weinberger, and J. Voitländer, Phys. Rev. B **50**, 2104 (1994).

[22] We avoid taking the limit as $n$ goes to infinity as this leads to some mathematical complications.

[23] H. E. Camblong and P. M. Levy (private communication).

[24] *Metals: Electronic Transport Phenomena*, edited by J. Bass, K. H. Fischer, K. Hellwege, and H. Olsen, Landolt-Bornstein, New Series, Vol. 15a, (Springer-Verlag, Berlin, 1982), pp. 176–178. We thank Jack Bass for this information. He adds that the equilibrium solubility of Co in Cu is low, so it is hard to be sure of any experimental result.

[25] J. Zabloudil, C. Uiberacker, C. Blaas, U. Pustogowa, L. Szunyogh, C. Sommers, and P. Weinberger, Phys. Rev. B **57**, 7804 (1998).

[26] C. Blaas, P. Weinberger, L. Szunyogh, P. M. Levy, C. B. Sommers, and I. Mertig, Philos. Mag. B **78**, 549 (1998).

[27] I. Mertig and P. Zahn (private communication).

[28] P. M. Levy, K. Ounadjela, S. Zhang, Y. Wang, C. B. Sommers, and A. Fert, J. Appl. Phys. **67**, 5914 (1990).

[29] P. M. Levy, H. E. Camblong, Z. P. Shi, and S. Zhang, *Magnetism and Structure in Systems of Reduced Dimensions*, NATO ASI Series B, Phyiscs, Vol. 309, edited by R. F. C. Farrow *et al.* (Plenum, New York, 1993), p. 155.

[30] C. Blaas, P. Weinberger, L. Szunyogh, J. Kudrnovský, V. Drchal, P. M. Levy, and C. Sommers, Eur. Phys. J. B (to be published).